Fuel Processing Technology 237 (2022) 107469

Contents lists available at ScienceDirect

Fuel Processing Technology

journal homepage: www.elsevier.com/locate/fuproc

Experimental study on the structure and reactivity of char in pressurized O_2/H_2O atmosphere

Chenxi Bai, Yu Zhang, Wenda Zhang, Kun Chen, Lihua Deng, Yijun Zhao *, Shaozeng Sun, Dongdong Feng *, Jiangquan Wu

School of Energy Science and Technology, Harbin Insitute of Technology, Harbin 150001, China

ARTICLE INFO

Keywords:
Char
O_2/H_2O
Pressurization
Structure
Reactivity

ABSTRACT

Pressurized O_2/H_2O combustion is regarded as a promising high-efficiency CCS technology. In this study, char combustion in a pressurized O_2/H_2O atmosphere was performed with a pressurized horizontal tube furnace. The effects of pressure (0.1–1.3 MPa) and H_2O concentration (0–60%) on char conversion, char physicochemical structure and reactivity were investigated by means of XPS, Raman, temperature-programed desorption and TGA tests. The results show that both pressurization and H_2O can promote char conversion and facilitate the formation of carbon-oxygen bonds on the char surface. Pressure mainly affects the consumption and generation of micropores, while the effect of H_2O on the pore structure has no obvious selectivity. Pressurization reduces the relative content of C—C, while H_2O has the opposite effect. At low pressure (0.1–0.7 MPa) and low H_2O concentration (0–40%), pressurization and H_2O can promote the formation of C(O) on the surface of char. The reactivity of char first decreased and then increased with increasing pressure and increasing H_2O concentration.

1. Introduction

CO_2 capture and storage technology has received extensive attention for the purpose of coping with climate change [1,2]. Major countries in the world have proposed carbon neutrality goals [3]. In China, coal-fired power plants are the largest source of CO_2 emissions [4]. Although the utilization of non-fossil energy has been paid attention, coal-fired power generation will still exist for a long time as a guarantee of energy security [5]. In the context of carbon neutrality, CO_2 capture during coal combustion has become a research focus. For new coal-fired units, oxy-fuel combustion technology is one of the effective CO_2 capture technologies, which can effectively increase the CO_2 concentration in the exhaust gas. For the purpose of achieving near-zero emissions from fossil fuels, Solvador [6,7] proposed the latest third-generation oxy-fuel combustion technology, namely O_2/H_2O combustion. This technology uses H_2O with a higher radiation than CO_2 to enhance heat exchange in the combustion chamber, and the high specific heat capacity to modify the flame temperature. At the same time, the phase transition of H_2O is used to remove impurities and obtain high concentration of CO_2. Conventional oxy-fuel combustion technology is carried out at atmospheric pressure, but in the oxy-fuel combustion power generation system, the air separation unit before combustion and the gas treatment device after combustion are all in high-pressure operation [8–10]. The process of changing system pressure leads to energy waste [11]. Besides, the recovery of latent heat from steam in flue gas can be possible, and the components will be smaller, leading to reductions in capital cost [12]. Therefore, the gasification-combustion reaction of coal under pressurized O_2/H_2O is of great significance.

At high temperature, H_2O can promote the combustion of coal. As a gasification agent, H_2O reacts with char to promote a large amount of CO and H_2 precipitation and promote homogeneous combustion [13]. At the same time, the H and OH radicals formed on the surface of char by H_2O can reduce the activation energy of char heterogeneous reaction [14]. The thermochemical transformation properties of char are closely related to its physicochemical structure [15,16]. Under the condition of O_2/H_2O, the char-H_2O gasification reaction occurs on the outer surface of the inner pores of the char, which changes the pore physicochemical structure of the char particles and directly affects the combustion characteristics of the char [17]. Studies have shown that H_2O plays the role of opening micropores and expanding pores during the gasification reaction. At lower char consumption, H_2O opens the pores of the char and forms micropores [18]. In the case of high H_2O concentration or high carbon conversion rate, H_2O promotes the development of various pores and provides diffusion channels for the gases involved in the

* Corresponding authors.
E-mail addresses: zhaoyijun@hit.edu.cn (Y. Zhao), 08031175@163.com (D. Feng).

https://doi.org/10.1016/j.fuproc.2022.107469
Received 7 June 2022; Received in revised form 30 July 2022; Accepted 13 August 2022
Available online 23 August 2022

reaction [19,20]. Previous studies have found that for the pyrolysis process, pressurization will reduce the char reactivity [21–23]. In the gasification reaction, pressurization can significantly promote the char-H_2O gasification reaction [24]. Less attention has been paid to the reactivity of char in pressurized O_2/H_2O combustion. At present, only Zhao et al. [25] have conducted a reactivity test on the residual char of pressurized O_2/H_2O, but did not draw a link between the pressure and the char reactivity. They argue that the reactivity of char coupled the effects of pyrolysis and combustion processes on its structure.

During the gasification process, the combination of O atoms and C atoms forms various oxygen-containing functional groups on the surface of char to form active centers. However, during the reaction, its inherent oxygen-containing functional groups were released during char consumption as H_2O facilitated the unzipping of the benzene ring. The amount of oxygen-containing functional groups on the char surface is jointly determined by the consumption of intrinsic functional groups and the introduction of H_2O gasification reaction [18]. Under the action of O_2 and OH radicals, C(O) complexes are formed on the char surface, which is the precursor of the reaction site C_f. In the temperature-programmed desorption experiment, it was found that the gaseous product formed by the desorption of carbon-oxygen complexes formed on the surface of char in a steam atmosphere was mainly CO [26,27]. Studies have shown that the amount of carbon-oxygen complexes on the char surface is positively correlated with the reactivity of NO reduction [28–30]. H_2O can also affect the degree of char ordering by consuming amorphous carbon and dissociating product H radicals to induce polycondensation of benzene rings [31,32].

However, the current research is based on atmospheric pressure, and there is little exploration of the thermochemical conversion of char under a pressurized O_2/H_2O atmosphere. Our previous work focused on the effects of pressurized O_2/H_2O atmosphere on N conversion during Shenhua char combustion and Zhundong demineralized char's structure [25,33,34]. There are few reports on the evolution of char surface chemical structure under a pressurized O_2/H_2O atmosphere. Moreover, the mechanism of H_2O gasification reaction on char surface carbon-oxygen complexes and active sites under pressurized conditions is not precise. Therefore, based on a novel pressurized horizontal tube furnace, this study explored the effects of pressure and H_2O concentration on char conversion, char physicochemical structure evolution, carbon-oxygen complexes generation, and char reactivity.

2. Experimental samples and methods

2.1. Coal samples

The material is Shenhua bituminous coal with a particle size of 53–125 μm. Its proximate analysis and ultimate analysis results are shown in Table 1.

2.2. Experimental methods

The pressurized pyrolysis char was first prepared, and then it was burned under the corresponding pressure with an O_2/H_2O atmosphere. Pyrolysis and combustion experiments were carried out using a pressurized horizontal tube furnace system, as shown in Fig. 1.

The gas distribution system includes reaction gas, equilibrium gas, and protection gas. The reaction gas was premixed with deionized water, Ar, and O_2, heated until the water was in the gas phase, and passed into the reaction tube. The equilibrium gas was Ar, and the flow setting was the same as that of reaction gas to ensure the balance of pressure inside and outside the reaction tube to prevent it from rupturing. The protection gas was Ar used to purge at the connection seal between the pushrod and the furnace body to prevent air from being brought into the reaction tube during the propulsion process. The electric propulsion system can realize the rapid entry of sample from the low temperature area to the high temperature area for chemical reaction and from the high temperature area to the low temperature area to stop the reaction. The reaction time can be strictly controlled to facilitate process analysis of char combustion. The low temperature at the front end of the reaction tube was set as the initial position of the sample, position 0, the central position of the furnace constant temperature zone was set as position 1, and the cooling position at the rear end of the reaction tube was set as position 2. The length of the constant temperature zone is 200 mm, and the length of the quartz boat is 120 mm. The quartz boat loaded with the sample was pushed from position 0 to position 1 for 1.32 s. The residence time was defined as when the sample was on position 1 for chemical reaction. After the reaction, the quartz boat was pushed from position 1 to position 2 for cooling within 1.48 s. In the case of pressurized O_2/H_2O atmosphere, position 0, position 2 and the back-pressure valve were heated to 200 °C by heating cable to ensure that H_2O maintained the gas phase under pressurized conditions, and at the same time avoid chemical reaction of char due to excessive temperature. In the preparation process of pyrolysis char, the temperature was set to 1000 °C, the atmosphere was Ar, and the gas flow inside and outside the reaction tube was 2 L/min. A back-pressure valve was modified to set value (0.1/0.4/0.7/1.0/1.3 MPa) and remain stable. The pushrod was used to push the quartz boat to position 1, then position 2 when ultimately pyrolysis after 40 min. The obtained pressurized pyrolysis char was subjected to combustion experiments under the corresponding pressure to explore the effects of pressure and H_2O concentration (0/20/40/60%) on the char's combustion process, structure, and reactivity. The operating conditions are shown in Table 2. A quartz boat spread with a 500 mg char sample was placed at position 0, and the system was sealed. When the furnace temperature rose to 1000 °C and the H_2O preheating units to 200 °C, the water pump was started. A 2.49 L/min reaction gas of O_2/H_2O/Ar and an equal flow rate of Ar for equilibrium gas were introduced inside and outside the reaction tube. The volume fraction of O_2 in the reaction gas was 10%, the dilution gas was Ar, and the rest was H_2O with a set volume fraction. The motor was turned on after the pressure was increased to the set value and remained stable by modifying the back-pressure valve. The quartz boat was pushed from position 0 to position 1 for chemical reaction and then moved to position 2 after 120 s. After the reaction, the system was cooled, and the residual sample was removed.

Table 1
Proximate and ultimate analysis of coal.

Proximate Analysis (wt%)				Ultimate Analysis (wt%)				
M_{ad}	V_{ad}	A_{ad}	FC_{ad}	C_{ad}	H_{ad}	N_{ad}	S_{ad}	O_{ad}
4.14	27.84	9.15	58.87	71.99	4.16	1.26	0.36	8.94

Note: ad = air dry basis.

2.3. Char characterization

2.3.1. Pore structure analysis

The pore structure of char was measured by a surface area and porosimetry analyzer (ASAP 2460, Micromeritics, USA). N_2 was used as the adsorption medium, and the adsorption capacity was related to the relative pressure. Adsorption and desorption tests were carried out at −195.85 °C after degassing at 250 °C, and the isotherm adsorption-desorption curve with relative pressure between 0.01 and 0.978 was obtained. The BET method calculated the specific surface area, and the pore volume and pore size parameters were calculated by the BJH method.

2.3.2. Raman spectroscopy analysis

The carbon skeleton structure of char samples was measured by a Raman spectrometer (LabRAM HR Evolution, HORIBA, France). The laser wavelength was 532 nm, the scanning range was 3000–200 cm^{-1}, and the spectral resolution was 1.8 cm^{-1}. The 1800–800 cm^{-1} band

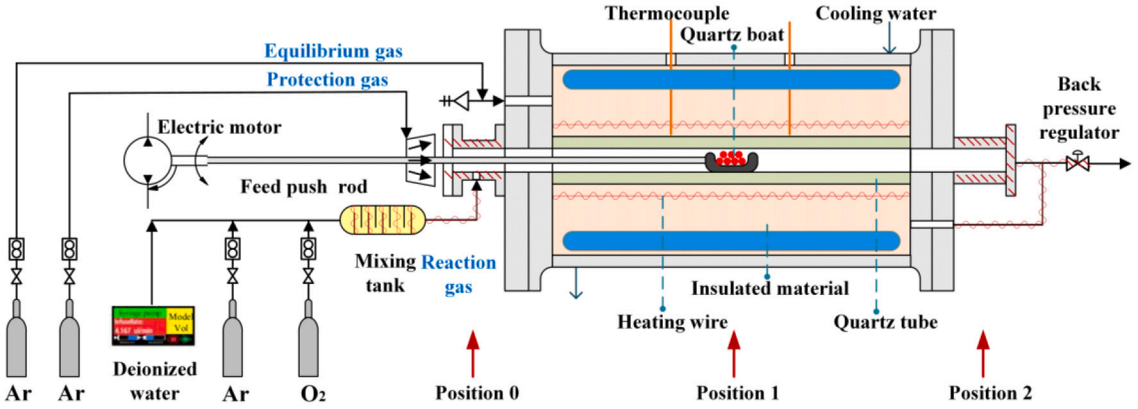

Fig. 1. Pressurized Horizontal Tube Furnace.

Table 2
Experimental conditions invested for char pressurized O_2/H_2O combustion.

No.	Pressure (MPa)	O_2 (%)	H_2O (%)	Ar (%)	Residence time (s)
1	0.1	10	20	70	120
2	0.4	10	20	70	120
3	0.7	10	20	70	120
4	1.0	10	20	70	120
5	1.3	10	20	70	120
6	0.7	10	0	90	120
7	0.7	10	40	50	120
8	0.7	10	60	30	120

curve was subjected to peak fitting processing.

2.3.3. X-ray photoelectron spectroscopy analysis

The bonding of C on the char surface was measured by X-ray photoelectron spectroscopy (ESCALAB 250Xi, ThermoFischer, USA). The excitation source was Al ka ray (hv = 1486.6 eV), the passing-energy was 30 eV, and the step size was 0.1 eV.

2.3.4. Temperature-programed desorption

The C(O) on the char surface was analyzed by TPD (temperature-programmed desorption) method [35]. A 20 mg sample of burning residual char in a pressurized O_2/H_2O atmosphere was placed in a N_2 atmosphere of 0.5 L/min, and the temperature was raised to 1200 °C at 5 °C/min to decompose the carbon-oxygen complexes on the char surface thermally. The corresponding C(O) content on the char surface was obtained.

2.3.5. Reactivity

The reactivity of the char was measured by a thermogravimetric analyzer (TGA/SDTA851^e, Mettler-Toledo, Switzerland). The mass of a single sample was 6 mg, and the flow was controlled at 20 mL/min. From room temperature to 500 °C stage, the carrier gas was N_2. After reaching 500 °C, it was switched to an atmosphere of 21% O_2 and 79% N_2, and the char burned out within 120 min.

2.3.6. Data processing

The equation for char conversion rate was shown in Eq. (1):

$$X = (m_0 - m)/[m_0(1 - X_{ash})] \times 100\% \quad (1)$$

where X is the conversion rate (%), m_0 is the mass of the original char sample (mg), m is the mass of the unburned char obtained at the residence time of 120 s (mg), and X_{ash} is the proportion of ash (%) in the char sample, which is obtained through the burnout experiment.

3. Results and discussion

3.1. Conversion rate of char

The effect of pressure (0.1/0.4/0.7/1.0/1.3 MPa) on char conversion was investigated at 1000 °C, 10% O_2, 20% H_2O, 70% Ar and 120 s residence time. The effect of H_2O on char conversion was studied at 0.7 MPa, 1000 °C, 10% O_2, and 120 s residence time. The char conversion rate under different pressure and H_2O conditions was shown in Fig. 2. It can be seen from Fig. 2a that as pressure was increased, the char conversion rate increased, and when the pressure increased from 0.1 MPa to 0.4 MPa, the char conversion rate increased by a larger amplitude, and then the pressure effect tended to be flat. This showed that the pressure effect promoted char-O_2/H_2O combustion. The increase in pressure promoted the adsorption of gas-phase reactants on the active sites of the char surface, thus increasing the reaction rate [36,37]. However, the increase in pressure led to a decrease in the pressure difference between the inside and outside of the char, which was not conducive to the outward diffusion of the gas generated inside the char, so the promotion effect of pressure on char conversion was weakened. As shown in Fig. 2b, the char conversion rate increased when H_2O concentration increased from 0% to 60%. Moreover, for every 20% increase in H_2O concentration, char will be about 15% consumed. The increase of H_2O strengthened char consumption in the gasification reaction [38,39].

3.2. Pore structure analysis

Fig. 3 shows the effect of pressure on the surface area and pores of char at 20% H_2O concentration. As shown in Fig. 3a, the External Surface Area increased when the pressure increased from 0.1 MPa to 0.7 MPa. However, it decreased when the pressure increased from 0.7 MPa to 1.3 MPa. Pressure had little effect on BET Surface Area and Micropore Area, but the contribution of micropores to the specific surface area (Micropore Area Ratio: Micropore Area / BET Surface Area) changed with the increase of pressure, and there was an inflection point. When the pressure increased from 0.1 MPa to 0.7 MPa, the Micropore Area Ratio decreased from 0.78 to 0.57, and when the pressure increased to 1.3 MPa, it increased to 0.71. As shown in Fig. 3b, when the pressure rose from 0.1 MPa to 0.7 MPa and 1.0 MPa, there were peaks in the change of pore volume and pore size, respectively. The pore volume reached the maximum at 0.7 MPa and 1.0 MPa, which are 0.195 cm^3/g. The pore size reached a maximum of 6.38 nm at 1.0 MPa. The influence of pressure on the physical structure of char was mainly reflected in the contribution of micropores to the pore structure. Pressurization promoted O_2 and H_2O enter the pores to consume micropores, transforming into mesopores and macropores, and expanding channels for gas [40]. Under 20% H_2O trial, the expansion of char's initial pores was fully developed at 0.7 MPa. Under this trial, the proportion of micropore area

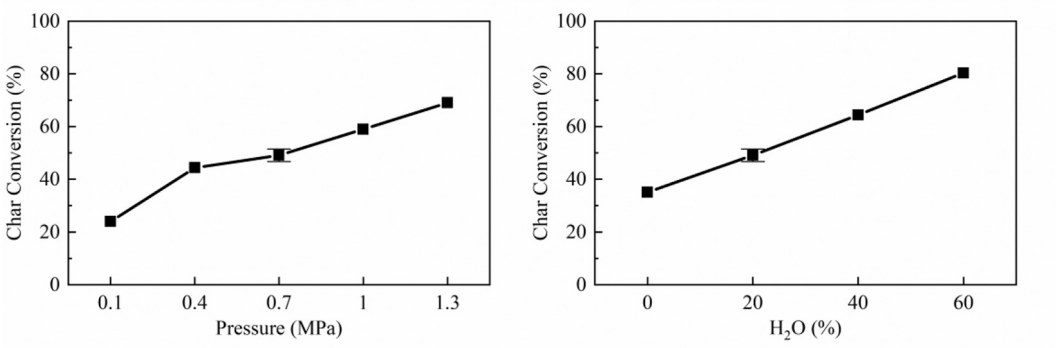

Fig. 2. Char conversion rate.

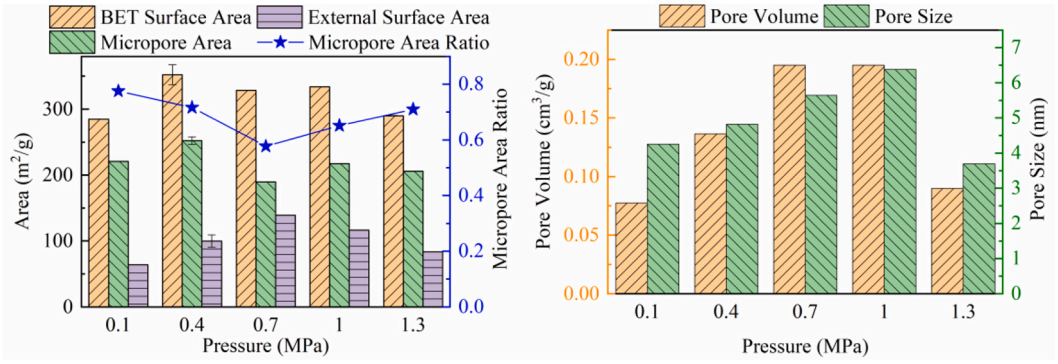

Fig. 3. Char physical structure under different pressures.

to the total reached the minimum, while the pore volume to the maximum. At higher pressures, the gasification reaction was significantly enhanced. The etching effect of H_2O opened pores on the char surface and expanded into narrow micropores [18,40].

Fig. 4 shows the effect of H_2O concentration on the physical structure of char at 0.7 MPa. As shown in Fig. 4a, the BET Surface Area and Micropore Area rose to peak values when the H_2O concentration was increased from 0% to 40%. When the H_2O concentration exceeded 40%, both BET Surface Area and Micropore Area decreased with the increasing H_2O. The peak value of the External Surface Area appeared at 20% H_2O concentration. When the H_2O concentration increased from 0% to >20%, the Micropore Area Ratio dropped from 0.79 to about 0.6 and remained stable. As shown in Fig. 4b, when the H_2O concentration increased from 0% to 20%, the pore volume was significantly increased from 0.047 cm^3/g to 0.19 cm^3/g. When the H_2O concentration exceeded 20%, the pore volume decreased slightly with the increase of H_2O. The H_2O concentration had little effect on the pore size.

Under pressurized conditions, the addition of H_2O promoted the diffusion of O_2 and the development of char pore structure. Tomków et al. [19] found that during char-H_2O gasification, the role of H_2O led to

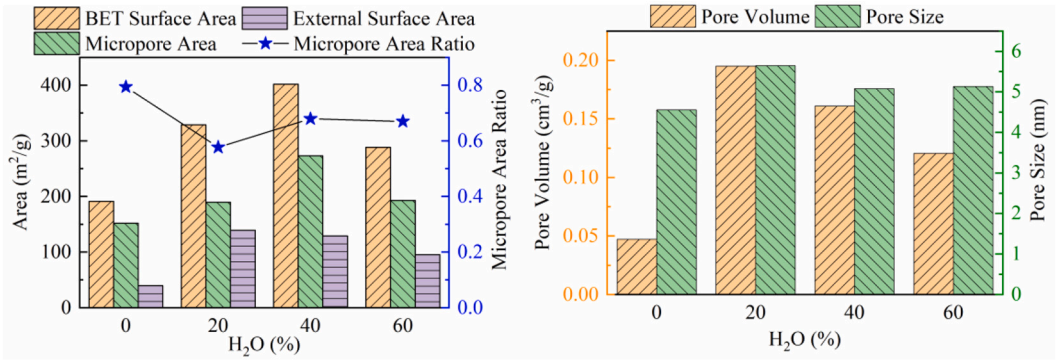

Fig. 4. Char physical structure under different H_2O concentration.

the development of various pore structures in char. This explained why the micropore area ratio and pore size were less affected by the H_2O concentration. The decrease in BET surface area under the 60% H_2O condition was due to the high char conversion.

3.3. Raman analysis

The skeleton structure of char was analyzed by Raman spectroscopy. According to previous studies [23], the Raman spectrum was fitted with 5 bands. The position and assignment of each sub-peak were shown in Table 3. Fig. 5 shows the curve fitting results by Peakfit of the sample obtained from 0.7 MPa, 20% H_2O concentration condition.

Parameters were calculated by the sub-peak area to characterize the structure of char, as shown in Fig. 6. I_{D1}/I_{D3} represents the ratio of large aromatic rings (>6) to small aromatic rings (3–5), I_G/I_{All} represents the relative content of graphitized structure, and I_{D1}/I_G for the defective structures. It can be seen from Fig. 6a that at 20% H_2O concentration, pressure had little effect on I_{D1}/I_G, while I_{D1}/I_{D3} and I_G/I_{All} decreased slightly with the increasing pressure. This indicated that in the O_2/H_2O atmosphere, the pressurization promoted the decomposition of large aromatic rings and decreased the degree of graphitization. Pressurization promoted the penetration of O_2 and H_2O to the inner surface of the char, resulting in the unzipping of the benzene ring structure. As shown in Fig. 6b, under 0.7 MPa, I_{D1}/I_{D3} was not significantly affected by H_2O. When the H_2O concentration increased, I_G/I_{All} rose in fluctuation, and I_{D1}/I_G decreased slightly. This was because the H radicals generated by the dissociation of H_2O under pressurized conditions can induce the polycondensation of the benzene ring so that the disordered carbon skeleton structure was gradually transformed into an ordered graphitization structure, the degree of aromatization and graphitization were improved [35,41].

3.4. XPS analysis

The species and relative contents of carbon, oxygen, and other elements on the char surface were obtained by peak fitting of XPS spectra. The deconvolution of C1s spectrum was divided into six sub-peaks, namely, sp^2 hybrid C—C peak, sp^3 bonded C—H peak of the carbon atom, hydroxyl/ether bond or carbon atom connected with internal lipid/ester bond C—O peak, carbonyl or carbon atom connected with two hydroxyl/ether bonds C═O peak, carboxyl or carboxylic anhydride O═C-O peak, and characteristic peak caused by aromatic or unsaturated structure π^*-π vibration transition [34,42]. Taking the XPS analysis of residual char under 0.7 MPa as an example, the peak position information and peak separation results of carbon-containing functional groups on char surface were shown in Fig. 7.

Fig. 8 summarizes the effect of pressure and H_2O on the bonding of carbon atoms on the char surface. As shown in Fig. 8a, in a 20% H_2O concentration atmosphere, with the increasing pressure, the C—C and C—H contents decreased slightly, the C—O and C═O contents increased steadily, and the O-C═O content fluctuated around 1.1%. The changes of C—C and C—H contents indicated that the pressure effect promoted the cracking of the aromatic ring structure by oxidizing substances [28], the degree of graphitization of char decreased, and the adsorption of reactants on the defect sites was strengthened, which promoted the cleavage of the C—H bond connected to the aromatic ring. The influence of pressure on the content of oxygen, phenolic hydroxyl, carbonyl, and carboxyl group on the surface of the char indicated that the pressure effect promoted the adsorption of oxygen on the surface of the char and constructed carbon-oxygen groups. However, unlike the increase in phenolic hydroxyl and carbonyl groups' content, carboxyl's stable content was due to its weak thermal stability and easy decomposition to generate CO_2. The weak fluctuation of its content was resulted from the coupling effect of pressure on the construction of carbon and oxygen groups and the promotion of combustion and decomposition. The effect of H_2O concentration on the carbon bonding on the char surface was investigated at 0.7 MPa. As shown in Fig. 8b, with the increasing H_2O concentration, the contents of C—C and C—O increased, while C—H decreased, while the rest have no apparent regularity. It showed that the adsorption reaction between H_2O and the defect structure on the char surface led to the consumption of the defect carbon structure and the deepening of the char's aromatization degree. The adsorption of char to form oxygen-containing intermediates was mainly phenolic hydroxyl groups.

Table 3
Parameters of fitted peaks from sample's Raman spectrum.

No.	Center (cm^{-1})	Assignment
D1	1350	Aromatic ring structure containing >6 benzene rings
D2	1620	Disordered graphite structure
D3	1530	Amorphous structure
D4	1200	Irregular arrangement of the carbon layer and the amorphous structure caused by the substituent group on the aromatic ring
G	1580	Regular graphite carbon structure with a C═C bond structure.

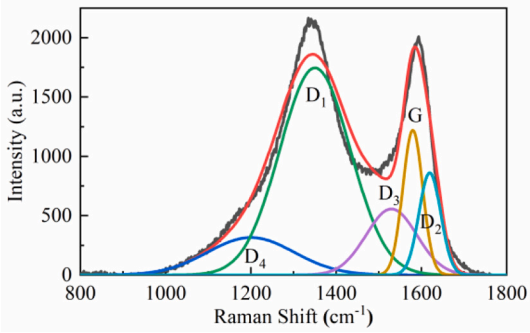

Fig. 5. Curve fitting of Raman spectrum.

3.5. TPD analysis

C(O) on the surface of char particles contains various kinds of functional groups, and their thermal stability are different [26]. In this study, the temperature in the constant temperature zone of the furnace was 1000 °C, while the char surface temperature was slightly higher than the ambient temperature during char-O_2/H_2O combustion [13]. Therefore, the final temperature of 1200 °C was set for TPD, and the amount of C(O) that was easy to participate in the reaction was explored. TPD was used to explore the effect of pressure under 20% H_2O concentration and H_2O concentration under 0.7 MPa on the amount of C(O) on the char surface. The results were shown in Fig. 9.

As shown in Fig. 9a, when the pressure increased from 0.1 MPa to 0.7 MPa, the amount of C(O) desorbed increased first and then decreased when the pressure increased to 1.0 MPa. Although the relative content of carbon-oxygen functional groups of 1.0 MPa and 1.3 MPa samples was relatively high in XPS analysis, the amount of desorbed C (O) in the TPD test was more petite, indicating that the proportion of easily decomposed carbon-oxygen functional groups were low below 1200 °C. As shown in Fig. 9b, when the H_2O concentration increased from 0% to 40%, the amount of C(O) increased significantly. H_2O can penetrate the inner layer of the char carbon matrix structure to promote the bond breaking between carbon and alkali metals and the formation of active functional groups on the char surface [43,44], and the etching effect of H_2O guides the formation of active sites on the char structure, providing active sites for oxygen adsorption. However, when the H_2O concentration reaches 60%, the amount of C(O) decreased to close to the 0% H_2O condition. This was because carbon's 120 s residence time conversion rate has reached 64.39% under 40% H_2O concentration. At this time, it began to enter the late stage of the reaction. Under 60% H_2O concentration, the char conversion rate was as high as 80.31%, and the

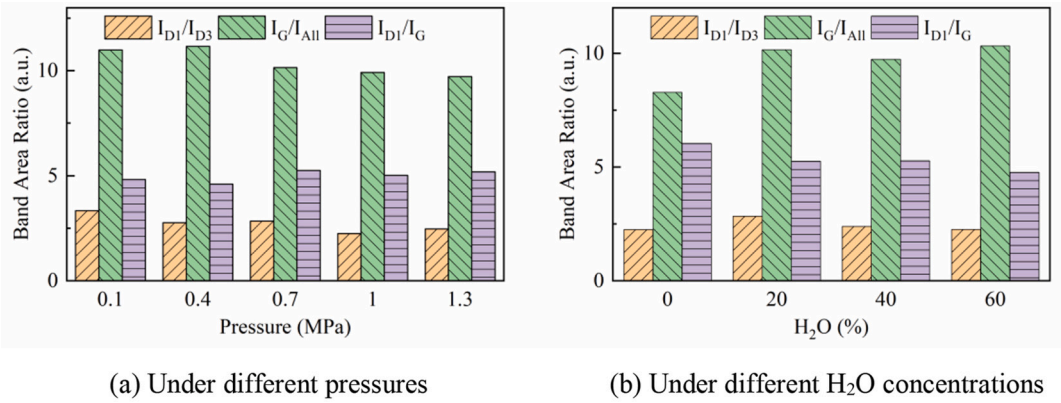

Fig. 6. Bands rotios of Raman parameters.

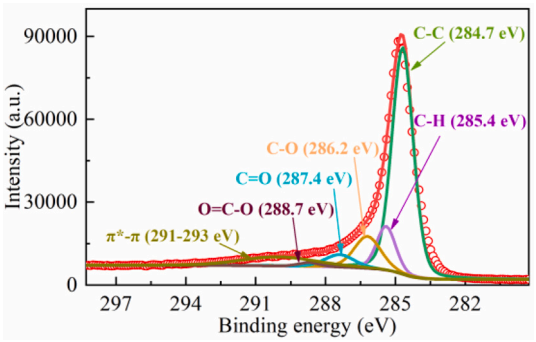

Fig. 7. Curve fitting of XPS C1s spectra acquired from char after combustion under pressurized O_2/H_2O atmosphere.

carbonization degree of char was high, the surface defect sites, aliphatic chains and bridge bonds were consumed, the pores collapsed and merged, the places that can provide active sites were reduced, so that the amount of C(O) on the char surface was reduced.

3.6. Reactivity analysis

The reactivity of char was tested by thermogravimetric analysis. In the above TPD experiments, it was found that CO was desorbed from the char surface at 600 °C. Therefore, the reactivity test was carried out at 500 °C to reduce the influence on char structure.

The char reaction rate at 30% and 50% char conversion and maximum reaction rate were analyzed. In order to explore the relationship between char structure and reactivity, the analysis was performed in the early stage of the reaction with a minor change in char structure. Among them, the maximum reaction rate of char occurs at the initial stage. It can be seen from Fig. 10a that at 20% H_2O concentration, when the pressure increased from 0.1 MPa to 1.0 MPa, the reactivity of char gradually decreased. When the pressure reached 1.3 MPa, the char reactivity increased. As shown in Fig. 10b, at 0.7 MPa, when the H_2O concentration increased from 0% to 40%, the char reactivity decreased, but when H_2O concentration increased to 60%, the reactivity increased. Zhang et al. [45] also found a similar phenomenon in char-H_2O gasification experiments. Raman analysis showed that H_2O promoted the graphitization degree of char and the consumption of defect structures, while pressurization decreased the graphitization degree of char and the decomposition of large aromatic rings. Besides, the development of char pore structure had no noticeable effect on the reactivity. It indicated that its carbon skeleton and physical structure did not determine the char reactivity. Zhao et al. [23] found that the amorphous carbon and defect structures in the pressurized pyrolysis char were consumed, and the reactivity decreased. The combustion of pressurized pyrolysis char in pressurized O_2/H_2O atmosphere was accompanied by an unsaturated reaction between char surface active sites and oxygen. Although in the char-O_2/H_2O in-situ reaction, the char reaction rate constant was proportional to the amount of C(O) complexes on the char surface [28]. However, in the ex-situ reactivity test, the empty active sites were generated by C(O) desorption. Therefore, the desorption of C(O) structures on the char surface was the rate-limiting step of the reaction.

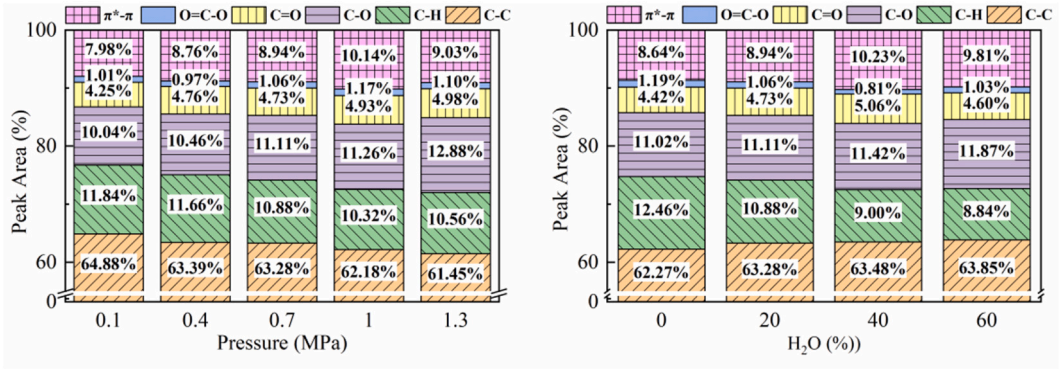

Fig. 8. Relative contents of surface functional groups determined from XPS C1s spectra.

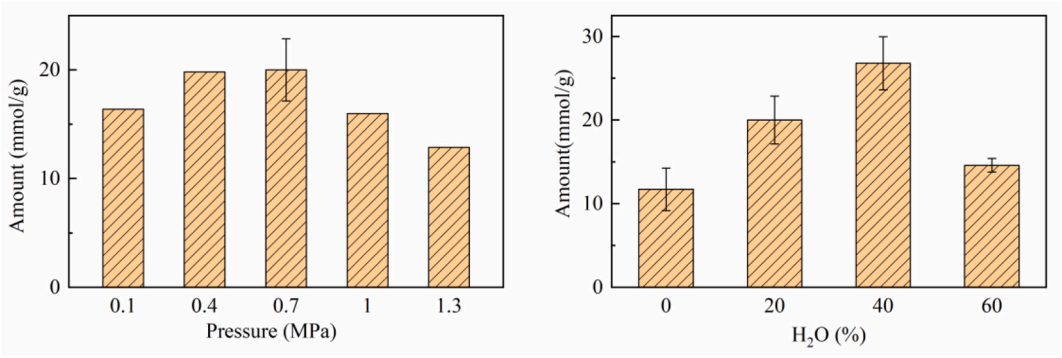

Fig. 9. Amount of C(O) on char surface.

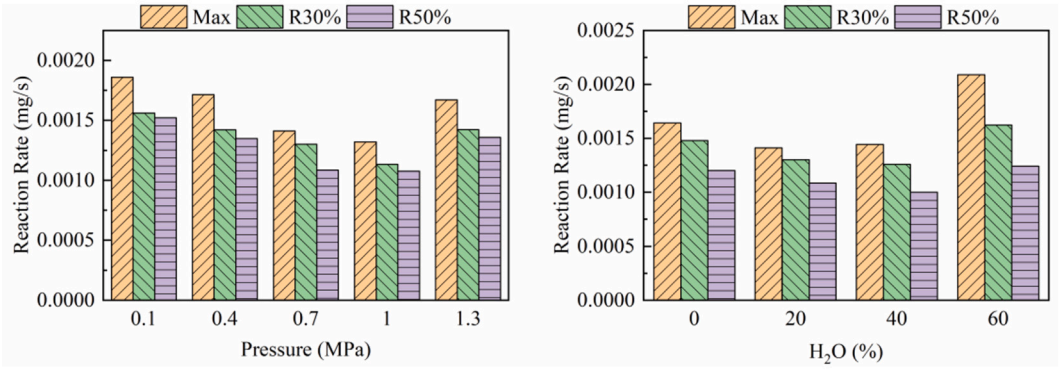

Fig. 10. Reactivity analysis of char.

4. Conclusions

1. Both pressurization and H_2O promote char-O_2/H_2O combustion, and the char conversion rate increased from 23.95% at atmospheric pressure to 69.07% at 1.3 MPa, with a significant increase at 0.4 MPa. Compared with the char conversion rate of 35.05% without H_2O, the char conversion rate increased by about 15% for every 20% increase in the H_2O concentration.
2. Pressure had a more apparent effect on micropores, while H_2O significantly affects various pores. Pressurization promoted the adsorption of oxygen on the surface of char, primarily when it increased from 0.1 MPa to 0.4 MPa, the aromatization degree of char decreased, and the content of phenolic hydroxyl, carbonyl, and aliphatic C—O on the surface increased. H_2O promoted the aromatization of char, the content of phenolic hydroxyl and carbonyl increased, and the content of C—H and aliphatic C—O decreased.
3. Under the relative low pressure (0.1–0.7 MPa), with the increase of pressure, the surface C(O) of char increased from 16.37 mmol/g to 20.00 mmol/g. At low H_2O concentration (0–40%), C(O) increased from 11.70 mmol/g to 26.78 mmol/g with the increase of H_2O concentration. The chemical structure of char played a major role in its combustion reactivity at low temperature.

Author statement

Chenxi Bai: Writing - original draft, Data curation, Investigation.
Yu Zhang: Investigation.
Wenda Zhang: Methodology.
Kun Chen: Investigation.
Lihua Deng: Investigation.
Yijun Zhao*: Project administration, Writing - review & editing.
Shaozeng Sun: Conceptualization.
Dongdong Feng*: Supervision.
Jiangquan Wu: Supervision.

Declaration of Competing Interest

The authors declare that they have no known competing financial interests or personal relationships that could have appeared to influence the work reported in this paper.

Data availability

Data will be made available on request.

Acknowledgements

Supported by the National Natural Science Foundation of China (51876050) and the Fundamental Research Funds for the Central Universities (2022ZFJH004).

References

[1] M. Bui, C.S. Adjiman, A. Bardow, E.J. Anthony, A. Boston, S. Brown, et al., Carbon capture and storage (CCS): the way forward, Energy Environ. Sci. 11 (2018) 1062–1176.

[2] B. Zhang, Y. Chen, B. Kang, J. Qian, X. Chuai, R. Peng, et al., Hydrogen production via steam reforming of coke oven gas enhanced by steel slag-derived CaO, Int. J. Hydrog. Energy 45 (2020) 13231–13244.

[3] Z. Jia, B. Lin, How to achieve the first step of the carbon-neutrality 2060 target in China: the coal substitution perspective, Energy. 233 (2021), 121179.

[4] Z. Li, S. Chen, W. Dong, P. Liu, L. Ma, J. He, Feasible and affordable pathways to low-carbon power transition in China, Clean Coal Technol. 27 (2021) 1–7.

[5] Z. Yang, D. Khatri, P. Verma, T. Li, A. Adeosun, B.M. Kumfer, et al., Experimental study and demonstration of pilot-scale, dry feed, oxy-coal combustion under pressure, Appl. Energy 285 (2021), 116367.

[6] C. Salvador, M. Mitrovic, K. Kourash, Novel Oxy-Steam Burner for Zero-Emission Power Plants, 2009.

[7] C. Salvador, Modeling design and pilot-scale experiments of CANMET'S advanced oxy-fuel/steam burner, in: International Oxy-combustion Reserch Network 2nd Workshop USA, 2007.

[8] L. Li, L. Duan, Z. Yang, Z. Sun, C. Zhao, Pressurized oxy-fuel combustion of a char particle in the fluidized bed combustor, Proc. Combust. Inst. 38 (2021) 5485–5492.

[9] W. Zhang, S. Sun, Y. Zhao, Z. Zhao, P. Wang, D. Feng, et al., Effects of total pressure and CO_2 partial pressure on the physicochemical properties and reactivity of pressurized coal char produced at rapid heating rate, Energy. 208 (2020), 118297.

[10] W. Zhang, S. Sun, H. Zhu, L. Zhang, Y. Zhao, P. Wang, The evolution characteristics of bituminous coal in the process of pyrolysis at elevated pressure, Fuel. 302 (2021), 120832.

[11] J. Hong, R. Field, M. Gazzino, A.F. Ghoniem, Operating pressure dependence of the pressurized oxy-fuel combustion power cycle, Energy. 35 (2010) 5391–5399.

[12] L. Chen, S.Z. Yong, A.F. Ghoniem, Oxy-fuel combustion of pulverized coal: Characterization, fundamentals, stabilization and CFD modeling, Prog. Energy Combust. Sci. 38 (2012) 156–214.

[13] K. Chen, W. Zhang, C. Bai, L. Deng, Y. Zhao, L. Zhang, et al., Modeling of single-particle char combustion under O_2/H_2O conditions: Effects of temperature and steam concentration, Fuel Process. Technol. 227 (2022), 107131.

[14] C. Wang, H. Shao, M. Lei, Y. Wu, L. Jia, Effect of the coupling action between volatiles, char and steam on isothermal combustion of coal char, Appl. Therm. Eng. 93 (2016) 438–445.

[15] D.J. Harris, I.W. Smith, Intrinsic reactivity of petroleum coke and brown coal char to carbon dioxide, steam and oxygen, Symp. Combust. 23 (1991) 1185–1190.

[16] K. Xu, S. Hu, S. Su, C. Xu, L. Sun, C. Shuai, et al., Study on Char Surface active Sites and their Relationship to Gasification Reactivity, Energy Fuel 27 (2013) 118–125.

[17] X. Guo, H.L. Tay, S. Zhang, C.-Z. Li, Changes in Char Structure during the Gasification of a Victorian Brown Coal in Steam and Oxygen at 800 °C, Energy Fuel 22 (2008) 4034–4038.

[18] M. Jasienkohalat, K. Kedzior, Comparison of molecular sieve properties in microporous chars from low-rank bituminous coal activated by steam and carbon dioxide, Carbon. 43 (2005) 944–953.

[19] K. Tomków, T. Siemieniewska, F. Czechowski, A. Jankowska, Formation of porous structures in activated brown-coal chars using O_2, CO_2 and H_2O as activating agents, Fuel. 56 (1977) 121–124.

[20] Y. Bai, P. Lv, X. Yang, M. Gao, S. Zhu, L. Yan, et al., Gasification of coal char in H_2O/CO_2 atmospheres: Evolution of surface morphology and pore structure, Fuel. 218 (2018) 236–246.

[21] E.S. Noumi, J. Blin, J. Valette, P. Rousset, Combined effect of Pyrolysis pressure and Temperature on the Yield and CO_2 Gasification Reactivity of Acacia Wood in macro-TG, Energy Fuel 29 (2015) 7301–7308.

[22] D. Lin, L. Liu, Y. Zhao, Y. Zhao, P. Qiu, X. Xie, et al., Influence of pyrolysis pressure on structure and combustion reactivity of Zhundong demineralized coal char, J. Energy Inst. 93 (2020) 1798–1808.

[23] W. Zhang, Y. Zhao, S. Sun, D. Feng, P. Li, Effects of pressure on the characteristics of bituminous coal pyrolysis char formed in pressurized drop tube furnace, Energy Fuel 33 (2019) 12219–12226.

[24] K. Matsuoka, D. Kajiwara, K. Kuramoto, A. Sharma, Y. Suzuki, Factors affecting steam gasification rate of low rank coal char in a pressurized fluidized bed, Fuel Process. Technol. 90 (2009) 895–900.

[25] L. Deng, W. Zhang, S. Sun, C. Bai, Y. Zhao, D. Feng, et al., Effect of pressure on the structure and reactivity of demineralized coal during O_2/H_2O thermal conversion process, Energy. 244 (2022), 122632.

[26] Z. Wang, R. Sun, Y. Zhao, Y. Li, T.M. Ismail, X. Ren, Investigation of demineralized coal char surface behaviour and reducing characteristics after partial oxidative treatment under an O_2 atmosphere, Fuel. 233 (2018) 658–668.

[27] L. Deng, Y. Zhao, S. Sun, D. Feng, W. Zhang, Review on thermal conversion characteristics of coal in O_2/H_2O atmosphere, Fuel Process. Technol. 232 (2022), 107266.

[28] Z. Wang, Y. Zhao, R. Sun, Y. Li, X. Ren, J. Xu, Effect of reaction conditions on the evolution of surface functional groups in O_2/H_2O combustion process of demineralized coal char, Fuel Process. Technol. 195 (2019), 106144.

[29] Z. Wang, L. Zhang, Y. Zhao, S. Feng, J. Ma, W. Kong, et al., Experimental investigation on the evolution characteristics of anthracite-N and semi-coke reactivity under various O_2/H_2O pre-oxidation atmospheres, Fuel Process. Technol. 216 (2021), 106725.

[30] S. Yue, C. Wang, Y. Huang, Z. Xu, J. Xing, E.J. Anthony, The role of H_2O in structural nitrogen migration during coal devolatilization under oxy-steam combustion conditions, Fuel Process. Technol. 225 (2022), 107040.

[31] D.M. Keown, J. Hayashi, C. Li, Drastic changes in biomass char structure and reactivity upon contact with steam, Fuel. 87 (2008) 1127–1132.

[32] C. Zou, L. Cai, D. Wu, Y. Liu, S. Liu, C. Zheng, Ignition behaviors of pulverized coal particles in O_2/N_2 and O_2/H_2O mixtures in a drop tube furnace using flame monitoring techniques, Proc. Combust. Inst. 35 (2015) 3629–3636.

[33] C. Bai, W. Zhang, L. Deng, Y. Zhao, S. Sun, D. Feng, et al., Experimental study of nitrogen conversion during char combustion under a pressurized O_2/H_2O atmosphere, Fuel. 311 (2022), 122529.

[34] L. Deng, W. Zhang, S. Sun, C. Bai, Y. Zhao, D. Feng, et al., Study on the thermal conversion characteristics of demineralized coal char under pressurized O_2/H_2O atmosphere, Fuel. 310 (2022), 122429.

[35] Z. Wang, R. Sun, Y. Zhao, Y. Li, X. Ren, Effect of steam concentration on demineralized coal char surface behaviors and structural characteristics during the oxy-steam combustion process, Energy. 174 (2019) 339–349.

[36] D. BJ, J. IA, The reaction of carbon with carbon dioxide at high pressure, Aust. J. Chem. 13 (1960) 194–209.

[37] S. Kajitani, N. Suzuki, M. Ashizawa, S. Hara, CO_2 gasification rate analysis of coal char in entrained flow coal gasifier, Fuel. 85 (2006) 163–169.

[38] Y. Zhao, D. Feng, B. Li, S. Sun, S. Zhang, Combustion characteristics of char from pyrolysis of Zhundong sub-bituminous coal under O_2/steam atmosphere: Effects of mineral matter, Int. J. Greenhouse Gas Control. 80 (2019) 54–60.

[39] Z. Zhang, B. Yi, Z. Sun, Q. Zhang, H. Feng, H. Hu, et al., Reaction process and characteristics for coal char gasification under changed CO_2/H_2O atmosphere in various reaction stages, Energy. 229 (2021), 120677.

[40] S. Kajitani, S. Hara, H. Matsuda, Gasification rate analysis of coal char with a pressurized drop tube furnace, Fuel. 81 (2002) 539–546.

[41] H.-L. Tay, S. Kajitani, S. Zhang, C.-Z. Li, Effects of gasifying agent on the evolution of char structure during the gasification of Victorian brown coal, Fuel. 103 (2013) 22–28.

[42] D. Feng, Q. Shang, H. Dong, Y. Zhang, Z. Wang, D. Li, et al., Catalytic mechanism of Na on coal pyrolysis-derived carbon black formation: Experiment and DFT simulation, Fuel Process. Technol. 224 (2021), 107011.

[43] D. Feng, Y. Zhao, Y. Zhang, Z. Zhang, L. Zhang, J. Gao, et al., Synergetic effects of biochar structure and AAEM species on reactivity of H_2O-activated biochar from cyclone air gasification, Int. J. Hydrog. Energy 42 (2017) 16045–16053.

[44] D. Feng, Z. Yu, Y. Zhao, S. Sun, J. Gao, Improvement and maintenance of biochar catalytic activity for in-situ biomass tar reforming during pyrolysis and H_2O/CO_2 gasification, Fuel Process. Technol. 172 (2018) 106–114.

[45] S. Zhang, Y. Luo, C. Li, Y. Wang, Changes in char reactivity due to char–oxygen and char–steam reactions using victorian brown coal in a fixed-bed reactor, Chin. J. Chem. Eng. 23 (2015) 321–325.